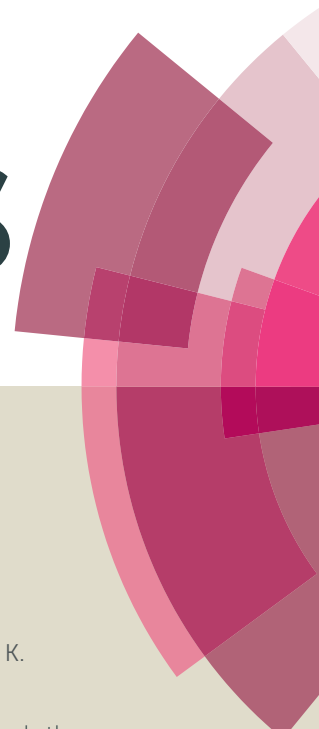


# RSC Advances



This article can be cited before page numbers have been issued, to do this please use: Y. Ding, Q. Wu, K. Zheng, L. An, X. Y. Hu and M. Wen-Jie, *RSC Adv.*, 2015, DOI: 10.1039/C5RA11127G.



This is an *Accepted Manuscript*, which has been through the Royal Society of Chemistry peer review process and has been accepted for publication.

*Accepted Manuscripts* are published online shortly after acceptance, before technical editing, formatting and proof reading. Using this free service, authors can make their results available to the community, in citable form, before we publish the edited article. This *Accepted Manuscript* will be replaced by the edited, formatted and paginated article as soon as this is available.

You can find more information about *Accepted Manuscripts* in the [Information for Authors](#).

Please note that technical editing may introduce minor changes to the text and/or graphics, which may alter content. The journal's standard [Terms & Conditions](#) and the [Ethical guidelines](#) still apply. In no event shall the Royal Society of Chemistry be held responsible for any errors or omissions in this *Accepted Manuscript* or any consequences arising from the use of any information it contains.

# Imaging of the nuclei of living tumor cells by novel ruthenium(II) complexes coordinated with 6-chloro-5-hydroxypyrido[3,2-a]phenazine

Yang Ding<sup>1</sup>, Qiong Wu<sup>1</sup>, Kangdi Zheng<sup>2</sup>, Linkun An<sup>3\*</sup>, Xiaoying Hu<sup>1</sup>, Wenjie Mei<sup>1\*</sup>

<sup>1</sup> School of Pharmacy, Guangdong pharmaceutical University, Guangzhou 510006, China.

<sup>2</sup> School of Tradition Chinese Medicine, Guangdong Pharmaceutical University, Guangzhou  
510006, China.

<sup>3</sup> School of Pharmaceutical Sciences, Sun Yat-sen University, Guangzhou 510006, China

## Abstract

Two novel ruthenium(II) complexes coordinated with 6-chloro-5-hydroxypyrido [3,2-a]phenazine (CQM),  $[\text{Ru}(\text{L})_2(\text{CQM})]\text{ClO}_4$  [L = 1,10-phenanthroline, (**1**) and 2,2'-bipyridine, (**2**)], were investigated as potent fluorescence probes to track the dynamic changes in the nuclei of living cells. Confocal laser technology was used to observe their co-location inside the cells. Results showed that both complexes were uptaken by HepG2 cells, especially for **1**, which was localized in the cell nuclei, whereas **2** was distributed in the cell nuclei and mitochondria. Further studies by real-time fluorescence observation revealed that **1** rapidly entered the living cells, namely, HepG2, HeLa and MCF-7 cells, imaged the dynamic in the nuclei of living tumor cells, and exhibited low toxicity to cells. Results demonstrated that **1** may be developed as a novel fluorescence probe for living cell nucleus. This study facilitates the development of fluorescence chemosensors with metal complexes.

**Keywords:** Ruthenium(II) complexes; 6-Chloro-5-hydroxypyrido[3,2-a]phenazine (CQM); Fluorescence probe; Nucleus; Living tumor cell

## 1. Introduction

Numerous studies have been performed to develop simple, sensitive, specific, and robust fluorescence probes/sensors for biochemistry, molecular biology, and clinical diagnostics.<sup>1</sup> Although many organic dyes have been designed and investigated, the utilization of these organic dyes is still limited because of their poor water solubility, low photo-stability, and high toxicity.<sup>2-5</sup>

To overcome the drawbacks of organic dyes, transition metal complexes, especially the versatile ruthenium(II) complexes, have increasingly attracted attention as potential fluorescence probes because of their wide spectral range, long-term luminescence and large Stokes shifts.<sup>6-10</sup> Several recent notable reviews have shown that luminescent ruthenium(II) complexes have emerged as promising candidates for wide application in chemosensors, biolabeling, in vivo tumor imaging, and live cell compartmentalization staining, such as in the nucleus, in the cytoplasm, in endosome, in mitochondria, in lysosomes and endoplasmic reticulum.<sup>11-16</sup>

Ruthenium complexes with dipyrrophenazine (dppz) ligands have been frequently investigated because of their strong DNA binding and their extraordinary photophysical properties.<sup>17,18</sup> In particular, these compounds have been paid much attention because of their “light switch effect”. These compounds are highly luminescent when intercalated into DNA and virtually nonemissive in aqueous solution, which is advantageous for fluorescence microscopy. For example, Barton et al. explored the cellular uptake of ruthenium(II) complexes and found that the complex cation  $[\text{Ru}(\text{DIP})_2(\text{DPPZ})]^{2+}$  (dip=4,7-diphenyl-1,10-

phenanthroline) is effectively transported into the cellular interior.<sup>19</sup> Furthermore, the mechanism of cellular entry of a luminescent ruthenium(II) polypyridyl complex  $[\text{Ru}(\text{DIP})_2(\text{DPPZ})]^{2+}$  was measured by flow cytometry and supported the passive diffusion of  $[\text{Ru}(\text{DIP})_2(\text{DPPZ})]^{2+}$  into the cell.<sup>20</sup> Rajendiran et al. also reported that a series of mixed ligand ruthenium(II) complexes  $[\text{Ru}(5,6\text{-dmp}/3,4,7,8\text{-tmp})(\text{diimine})]^{2+}$  as fluorescent probes for nuclear and protein components.<sup>21</sup>  $[\text{Ru}(\text{phen})_2(\text{DPPZ})]^{2+}$  has also been reported to be uptaken by cells and used as an efficient optical probe for staining nuclear components,<sup>22</sup> whereas ruthenium(II) complexes containing 7-F-dppz [7-fluorodipyrido (3,2-a:2',3'-c)phenazine] can be uptaken by cells and localize in the nucleus.<sup>23</sup> More recently, an alkyl ether chain has been bound into a dppz ligand, which increased the lipophilicity and membrane permeability of ruthenium(II) complexes.<sup>24,25</sup> In addition, ruthenium-octaarginine-conjugated polypyridyl peptides have been investigated.<sup>26,27</sup> Ruthenium(II) estradiol polypyridine complexes and dinuclear ruthenium(II) complexes have also been considered as probes for cellular imaging.<sup>28-31</sup> However, there are still few agents succeed in direct staining nuclear ascribe to their poor membrane permeability, poor cellular uptake and high toxicity, and it's remains a huge challenge to develop novel fluorescence probe of living cells. Thus, imaging of living cells is still challenging because of the high toxicity, limited uptake in living cells, and limited nuclear accumulation of these complexes under investigation.

Studies were performed to target metal complexes to the nucleus more effectively. Two novel ruthenium(II) complexes coordinated with CQM,  $[\text{Ru}(\text{L})_2(\text{CQM})]^{2+}$ , [1,10-

phenanthroline, (**1**) and 2,2'-bipyridine, (**2**)] (Scheme 1), were synthesized under microwave irradiation, and their properties on imaging of the nuclei of living tumor cells were investigated.

**Scheme 1.** Molecular structure of ruthenium(II) complexes **1** and **2**.

## 2. Experimental section

### 2.1 Materials and methods

All reagents were purchased from commercial suppliers without further purification. Solvents were dried and purified by conventional methods prior to using. Ruthenium chloride hydrate was obtained from Mitsuwa Chemicals. 8-Hydroxyquinoline was purchased from Aladdin. All the chemicals including solvents were obtained from commercial vendors and used as received. The Tris-KCl buffer consisted of Tris (10 mM) and NaCl (100 mM), and the pH value was adjusted to 7.2 with HCl (0.1 mol).

The complexes were synthesized using Anton Paar Monowave 300 microwave reactor (an initiator single mode microwave cavity at 2450 MHz, Biotage).  $^1\text{H}$  NMR and  $^{13}\text{C}$  NMR spectra were recorded on a Bruker DRX 2500 spectrometer in  $d^6$ -DMSO, and the electrospray ionisation mass spectrometry (ESI-MS) spectra were obtained in acetonitrile on an Agilent 1100 ESI-MS system operating. The electronic absorption spectra were recorded on a Shimadzu UV-2550 spectrophotometer, the steady-state emission spectra were recorded

on a RF-5301 fluorescence spectrophotometer. Fluorescence images of cellular localization were obtained using EVOS® FL Auto Imaging System. Living-Cell Confocal imaging was performed with an Zeiss LSM 510 META.

## 2.2 Synthesis and Characterization

6,7-dichloroquinoline-5,8-dione (DCQ) was prepared by using a similar method to that was reported in the literature.<sup>32</sup> In general, a mixture of 8-Hydroxyquinoline (45 mmol, 6.5 g), NaOH (25 mmol, 10 g), NaClO<sub>3</sub> (28 mmol, 3 g) and high concentration hydrochloric acid (150 ml) was heated at 80 °C for 3 h, the products were obtained by on-step column chromatography of silica-gel. Yields, 65%. <sup>1</sup>H NMR (500 MHz, DMSO-d<sub>6</sub>): δ 9.05 (dd, J = 4.6, 1.6 Hz, 1H), 8.46 (dd, J = 7.9, 1.6 Hz, 1H), 7.90 (dd, J = 7.9, 4.7 Hz, 1H) (Fig. S3). 6-Chloro-5-hydroxypyrido[3,2-a] phenazine (CQM) was synthesized according to the literature with some improvement.<sup>33</sup> In general, a mixture of 6,7-dichloroquinoline-5,8-dione (1 mmol, 0.23 g) and o-Phenylenediamine (1.2 mmol, 0.13 g) in 20 ml of ethanol was heated at 95 °C for 30 min under microwave irradiation. The yellow precipitate was obtained by filter while it's hot and washed with ethanol, then dried in vacuo. Yield: 37%. ESI-MS (in chloroform): *m/z* 282.5 (Fig. S4).

### Synthesis of [Ru(phen)<sub>2</sub>(CQM)](ClO<sub>4</sub>)<sub>2</sub> (1)

A mixture of CQM (0.6 mmol, 165 mg) and cis-[Ru(phen)<sub>2</sub>Cl<sub>2</sub>]-H<sub>2</sub>O (0.4 mmol, 228 mg) in Ethylene glycol (20 mL) was heated at 140 °C for 30 min under microwave irradiation. After cooled to room temperature, the mixture was stirred for 3 min with the addition of excess saturated NH<sub>4</sub>PF<sub>6</sub> solution. The orange products were obtained by filter

and purified by on-step column chromatography of silica-gel (166 mg, 73%), ESI-MS (in acetonitrile):  $m/z$  742.2.  $^1\text{H}$  NMR (500 MHz,  $d^6$ -DMSO):  $\delta$  9.10 (d,  $J = 5.2$  Hz, 1H), 8.87-8.70 (m, 3H), 8.58 (dd,  $J = 11.6, 8.5$  Hz, 2H), 8.48 (d,  $J = 4.5$  Hz, 1H), 8.43-8.27 (m, 5H), 8.23 (t,  $J = 9.9$  Hz, 1H), 8.15-8.04 (m, 4H), 8.03-7.93 (m, 2H), 7.88 (dt,  $J = 7.4, 5.2$  Hz, 2H), 7.82-7.72 (m, 2H), 7.62 (ddd,  $J = 8.2, 6.8, 3.9$  Hz, 3H).  $^{13}\text{C}$  NMR (126 MHz, DMSO),  $\delta$  167.46 (s), 154.77 (s), 153.48 (s), 152.35 (s), 152.05-151.78 (m), 149.88 (s), 149.88 (s), 148.76 (s), 148.69 -148.59 (m), 148.40 (s), 147.91 (s), 147.91 (s), 143.52 (s), 142.91 (s), 138.72 (s), 137.49 (s), 136.82 (s), 136.59-136.48 (m), 136.45 -136.36 (m), 136.16-135.97 (m), 135.42 (s), 133.53-133.36 (m), 131.92-131.78 (m), 131.12 (s), 130.83 (s), 130.62 (s), 129.76-129.69 (m), 127.56 (s), 127.00-126.95 (m), 126.92-126.82 (m), 126.75 (s), 126.51 (s), 126.13 (s), 125.71 (s), 112.67 (s).

### Synthesis of $[\text{Ru}(\text{byp})_2(\text{CQM})](\text{ClO}_4)_2$ (2)

A mixture of CQM (0.184 mmol, 50 mg) and  $\text{cis-}[\text{Ru}(\text{bpy})_2\text{Cl}_2]\cdot\text{H}_2\text{O}$  (0.115 mmol, 80 mg) in ethylene glycol (20 mL) was heated at 140 °C for 30 min under microwave irradiation. After cooled to room temperature, the mixture was stirred for 3 min with the addition of excess saturated  $\text{NH}_4\text{PF}_6$  solution. The orange products were obtained by filter and purified by on-step column chromatography of silica-gel (60 mg, 75%), ESI-MS (in acetonitrile):  $m/z$  694.2.  $^1\text{H}$  NMR (500 MHz,  $d^6$ -DMSO):  $\delta$  9.40 (dd,  $J = 8.2, 1.3$  Hz, 1H), 8.76 (ddd,  $J = 56.4, 35.8, 6.5$  Hz, 5H), 8.22 (dd,  $J = 8.5, 0.9$  Hz, 1H), 8.11 (t,  $J = 8.0$  Hz, 3H), 8.04 (dtd,  $J = 19.0, 8.0, 1.4$  Hz, 2H), 7.97 (t,  $J = 7.5$  Hz, 1H), 7.93-7.81 (m, 2H), 7.83-7.71 (m, 3H), 7.72-7.64 (m, 1H), 7.53 -7.34 (m, 3H).  $^{13}\text{C}$  NMR (126 MHz, DMSO),  $\delta$  167.10 (s),

159.31 (s), 158.22 (s), 157.94 (s), 157.69 (s), 153.49 (s), 152.64 (s), 152.29 (s), 152.05 (s), 151.54 (s), 150.57-150.33 (m), 143.54 (s), 142.87 (s), 138.73 (s), 172.86-109.61 (m), 175.64-100.01 (m), 137.57 (s), 137.43 (s), 137.22 (s), 136.71 (s), 136.47 (s), 133.45 (s), 131.89 (s), 129.72 (s), 128.82 (s), 128.77 (s), 128.08 (s), 128.00 (s), 127.79 (s), 127.56 (s), 127.47 (s), 125.83 (s), 124.91 (s), 124.66 (s), 124.54 (s), 124.41 (s), 112.74 (s).

### 2.3 Cell lines and cell culture

Human cancer cell lines, including the HepG2 (hepatocellular carcinoma cell line), HeLa (cervical carcinoma cell line), and MCF-7 (breast carcinoma cell line) were purchased from American Type Culture Collection (ATCC, Manassas, VA). The normal HaCaT (immortalized human epidermal cell line) also obtained from ATCC. All cell lines were cultured in 25 cm<sup>2</sup> culture flasks in DMEM medium (Gibco, Gaithersburg, MD, USA) supplemented with fetal bovine serum (10%), penicillin (100 U/mL), and streptomycin (50 U/mL) at 37 °C in a CO<sub>2</sub> incubator (95% relative humidity, 5% CO<sub>2</sub>).

### 2.4 Cellular localization

The cells were cultured in DMEM medium supplemented with 10% Fetal Bovine Serum (FBS) at 37 °C and 5% CO<sub>2</sub>. Cells in complete growth medium at  $2 \times 10^6$  cells per mL were incubated for 24 h at 37 °C, unless otherwise stated. Cells were washed by PBS and then treated with ruthenium(II) complexes **1** and **2** (200 μM) in DMSO/PBS (pH 7.2, 1:99, v/v) for 2 h at 37 °C and 5% CO<sub>2</sub>, respectively. Then cells were stained with Hoechst 33258 and Mito-tracker green FM for another 20 min and finally luminescence imaging by confocal microscope.

## 2.5 Cytotoxicity assay

The *in vitro* cytotoxicity of the ruthenium(II) complexes **1** and **2** toward HepG2, HeLa, MCF-7, and HaCaT cells have been studied by the 3-(4,5-Dimethylthiazole)-2,5-diphenyltetraazolium bromide (MTT) assay. Cells were incubated with different concentrations (0, 25, 50, 100, 150, 200  $\mu$ M) of complexes for 24 h. Cell viability was determined by measuring the ability of cells to transform MTT into a purple formazan dye, which was carried out as described previously. Cells were seeded in 96-well tissue culture plates for 24 h. After incubation, 20  $\mu$ L per well of MTT solution (5 mg/mL phosphate buffered saline) was added and incubated for 4 h. The color intensity of the formazan solution, which reflects the cell growth conditions, was measured at 490 nm using a microplate spectrophotometer (SpectroAmaxt 250). All data were from at least three independent experiments and are expressed as the mean  $\pm$  the standard deviation. The following formula was used to calculate the viability of cell growth:

$$\text{Viability (\%)} = \left( \frac{\text{mean of Absorbance value of treatment group}}{\text{mean Absorbance value of control}} \right) \cdot 100$$

## 2.5 Real-time fluorescence images

The cells were grown in DMEM medium supplemented with 10% Fetal Bovine Serum (FBS) at 37 °C and 5% CO<sub>2</sub>. Cells ( $2 \times 10^6$ ) were seeded in 75 cm<sup>2</sup> culture flasks for 12 h before imaging. The cells were incubated with the Hoechst 33258 for 10 min at 37 °C under 5% CO<sub>2</sub> followed by carefully washing cells with PBS solution and then incubated with the complexes **1** and **2** (200  $\mu$ M), respectively. At last, the cells were monitored with

fluorescence microscopy to obtain real-time fluorescence images every 5 min.

## 2.6 Cellular uptake of complexes 1 and 2

The cells were cultured DMEM medium supplemented with with 10% Fetal Bovine Serum (FBS) at 37 °C and 5% CO<sub>2</sub>. After 24 h incubation, the cells were washed with PBS and then the cell culture medium of the cell culture flasks was replaced to 10 mL of the cell culture medium solutions containing the complexes 1 and 2 (50 μM) and the flasks were incubated at 37 °C, 5% CO<sub>2</sub> for 6 h. The UV-Vis spectra of the solutions in HepG2, HeLa and MCF-7 cells treated with complexes 1 and 2 were tested every one hour, respectively.

## 2.7 Amphiphilicity measurement

The lipo-hydro partition coefficient of the complexes was tested by using octanol-water two-phase system. In general, equal amounts of octanol and distilled water were thoroughly mixed in the oscillator for 24 h, then separate two-phase solution. Complexes were carefully dissolved in water phase and octanol phase for 20 μM solution with sufficient mixing. After separation, the final concentration of the water phase was denoted as C<sub>w</sub> and the concentration of the octanol phase denoted as C<sub>o</sub>. Both C<sub>o</sub> and C<sub>w</sub> were tested by ultraviolet-visible (UV-vis) spectrophotometer, and the partition coefficient (P<sub>o/w</sub>) for the complex was calculated according to the equation:  $P_{o/w} = A_o/A_w$ .

## 3. Results

### 3.1 Synthesis and characterization

Targeted complexes 1 and 2 were synthesized under microwave irradiation at 140 °C for 30 min with corresponding yields of 73% and 75%. The complexes were purified by

chromatography. The chemical structures of the two ruthenium(II) complexes were further confirmed by ESI-MS (Fig. S5). The mass spectra in acetonitrile exhibited a peak at  $m/z$  742.2 (100%) for **1** and 694.2 for **2** (100%) which was ascribed to  $[M-ClO_4^- - H^+]^+$  and agreed with the theoretical value. The chemical shifts ( $\delta$ ) of the  $^1H$  NMR spectra of **1** (Fig. S6), which were attributed to the protons of each phenanthroline ligand of  $H_1$ ,  $H_2$ ,  $H_3$ ,  $H_4$  and  $H_5$ , appeared at 9.10, 8.79, 8.55, 8.45, and 8.35 ppm, respectively. The chemical shifts attributed to the phenazine ring  $H_a$ ,  $H_b$ ,  $H_c$ ,  $H_d$  and  $H_e$  appeared at 8.35, 7.76, 7.97, 7.83, and 7.62 ppm, respectively. The chemical shifts ( $\delta$ ) of the  $^1H$  NMR spectra of **2**, which were attributed to the protons for each bipyridyl ligand of  $H_1$ ,  $H_2$ ,  $H_3$ , and  $H_4$ , appeared at 8.22, 7.44, 7.97 and 8.76 ppm, respectively. The chemical shifts attributed to the phenazine ring  $H_a$ ,  $H_b$ ,  $H_c$ ,  $H_d$ , and  $H_e$  appeared at 8.54, 7.76, 7.97, 8.04, and 7.71 ppm, respectively.

To date, microwave irradiation, as an alternative heat source, is becoming increasingly popular in chemistry because this preparation method is simple and facilitates rapid heating and cooling, concurrent heating and cooling, and energy efficient “green” synthesis with low-boiling solvents at high temperature in closed vessels.<sup>34–36</sup> Target compounds **1** and **2** were prepared by microwave-assisted synthesis technology.<sup>37–42</sup> The temperature of the reaction system instantly reached 140 °C for 30 min under microwave irradiation, which was maintained during the whole process (Fig. S2). The corresponding yields for **1** and **2** under microwave irradiation were approximately 73% and 75%.

### 3.2 Photophysical properties of complexes **1** and **2**

The fluorescence properties of the two ruthenium complexes in different solvents was

investigated. Complexes **1** and **2** resolved in EtOH, DMEM, and PBS were irradiated under ultra light (365 nm) to observe their emission fluorescence. Complex **1** exhibited stronger red fluorescence than **2**, and this fluorescence was not quenched by water, contrary to some compounds with very weak fluorescence because their fluorescence can be quenched by water (Fig. 1A). The electronic absorption spectra of **1** and **2** (100  $\mu$ M) in Tris-KCl buffer solution (pH 7.2) exhibited characterized MLCT transition absorption at 500 and 450 nm, respectively. In addition, the characterized intraligand ( $\pi \rightarrow \pi^*$  charge transition) absorption for complexes **1** and **2** appeared at 260 and 300 nm, respectively (Fig. 1B). In the emission fluorescence spectra, when excited at 400 nm, **1** exhibited strong fluorescence in the range of 500–700 nm, with the maximum intensity of 290 at 590 nm. For **2**, only a weak fluorescence with the maximum intensity of 30 appeared at around 580 nm (Fig. 1B). These results suggested that compound **1** coordinated with phen exhibited stronger fluorescence than **2** coordinated with bpy, which confirmed that coplanar molecules have stronger conjugation effects on enhancing fluorescence emission.

### 3.3 Cellular uptake and distribution

The cellular distributions of complexes **1** and **2** were confirmed using confocal laser scanning microscopy. The nuclei of HepG2 cells were stained blue using Hoechst 33258, whereas the mitochondria were stained green using Mito-tracker green FM. After treatment with **1** (100  $\mu$ M) for 2 h, strong fluorescence ascribed to the **1** was observed in the nucleus, which was almost completely overlaid with that of Hoechst 33258, and not overlaid with that of Mito-tracker green FM. For **2**, the fluorescence was not only overlaid with Hoechst 33258,

but also with Mito-tracker green FM (Fig. 1C). Further a cross sectional compositional line profile of a single cell emission intensity from each probe clearly showed superimposed emissions of **1** and Hoechst 33258 in a single cell, and confirming that they co-localized (Fig. 1D). Remarkably, these data indicated that **1** localized mainly in the nuclei, whereas **2** accumulated in the mitochondria and nuclei of HepG2 cells.

### Figure 1

Thus, the cellular uptake and distribution by HepG2, HeLa, and MCF-7 cells were further confirmed. After treatment with either **1** or **2** ( $[\text{Ru}] = 200 \mu\text{M}$ ) for 2 h, both complexes were confirmed to be uptaken by all cells (Figs. 2A–C). The luminescence intensity of complexes **1** and **2** in the HepG2, HeLa, and MCF-7 are shown in Figs. 2a–c. The results showed that the luminescence intensity of **1** was stronger than that of **2** in tumor cell fluorescence imaging.

### Figure 2

#### 3.3 Low cytotoxicity of ruthenium(II) complexes against various cells

Low cytotoxicity against the growth of various cells of both complexes was confirmed using MTT assay. We examined the various cells in vitro cytotoxicities of these ruthenium(II) complexes **1** and **2** against HepG2, HeLa, MCF-7 and HaCaT cells by using

MTT assay. All cells were treated with varying concentrations of ruthenium(II) complexes at 37 °C for 24 h to explore their antitumor potential, and cell viability was determined by MTT assay. After 24 h of treatment with either **1** or **2** at 200 μM, no significant cytotoxic response was observed for HepG2, HeLa, MCF-7, and HaCaT cells for **1** and **2**. The viability for **1** in the HepG2, HeLa, MCF-7 and HaCaT cells were 87.2%, 78.5%, 68.1% and 66.9% respectively, after 24 h of incubation at 37 °C for 24 h. By contrast, the viability for **1** in the HepG2, HeLa, MCF-7 and HaCaT cells were 89.0%, 72.2%, 68.5% and 65.3% respectively, after 24 h of incubation at 37 °C for 24 h (Fig. 3). These results demonstrated that complexes **1** and **2** generally presented low toxicities for luminescence cell imaging under the applied conditions.

### Figure 3

#### 3.3 Imaging of the nuclei of living tumor cells by ruthenium(II) complexes

Finally, the efficiency of both complexes for imaging living tumor cells was determined. HepG2, HeLa, and MCF-7 cells were incubated with the two ruthenium(II) complexes at 37 °C, and the luminescence changes in both complexes were recorded every 5 min. Prior to incubation with the ruthenium(II) complexes, very weak luminescence was observed in the cells. After the cells were incubated with either **1** or **2**, a continuous bright luminescence gradually appeared in the cell after 20 min and reach to the strongest intensity was observed at 120 min (Figs. 4A–C). The red fluorescence spots showed that compounds **1**

and **2** were continuously entered the cell during incubation. The transfection rates for **1** in the HepG2, HeLa, and MCF-7 cells were approximately 95%, 100%, and 100%, respectively, after 2 h of incubation. By contrast, the transfection rates for **2** in the HepG2, HeLa, and MCF-7 cells were approximately 100%, 52%, and 67%, respectively, after 2 h of incubation (Figs. 4A–C). The results clearly indicated that **1** and **2** rapidly and selectively highlighted specific regions of living cells, leading to significant luminescence enhancement. Obviously, compound **1** entered cells faster than **2** and the transfection rate of **1** also exceeded that of **2**. Furthermore, the possible effectors of the cellular internalization process were investigated by evaluating the lipophilicities of ruthenium(II) complexes **1** and **2** using the octanol/water partition coefficient ( $\log P_{o/w}$ ). The measured partition coefficients of the ruthenium(II) complexes were 0.10 for **2** (lipophilic) to 0.18 for **1** (lipophilic) (Fig. 4G). Obviously, compound **1** is comparatively more lipophilic than **2**. In addition, UV-vis absorption spectra showed a decrease in the concentration of both complexes after the time elapsed in the cell culture medium of cells by UV-vis absorption spectra (Fig. S8-9). The fluorescence intensity of **1** increased faster and was stronger than that of **2** (Figs. 4D–F), which may be attributed to the higher lipophilic partition coefficients of **1** ( $\log P = 0.18$ ) than that of **2** ( $\log P = 0.10$ ).

#### Figure 4

#### 4 Discussion

Ruthenium(II) complexes have been designed and investigated as potential fluorescence

probes for cells, but they have not been successfully used in imaging of the nuclei of living cells.<sup>43</sup> The most promising complexes reported are polypyridine ruthenium(II) complexes coordinated with dppz, which is an enlarged aromatic ring intercalating ligand.<sup>17–18,44–46</sup> However, the utilization of these complexes is limited because of their high toxicity and low efficacy.<sup>27–28,45–49</sup> In the present study, two novel ruthenium(II) complexes coordinated with CQM, which mimics to the structure of dppz ligands, were synthesized and demonstrated by the highly efficient staining of the nuclei of different tumor cells. The cellular uptake of **1** and **2** by HepG2 cells was first confirmed by confocal laser scanning microscopy. Results showed that **1** localized in the nuclei of cells, whereas **2** accumulated in the nuclei and mitochondria. This phenomenon was further confirmed on other type of tumor cells, namely, HeLa, and MCF-7 cells. All cells were stained by either **1** or **2**. Thus, the toxicity of both complexes against various tumor cells was evaluated by MTT methods to determine whether both complexes can be used to probe living cells. As expected, both complexes exhibited low toxicity to HepG2, HeLa, MCF-7, and HaCaT cells even at a high concentration 200  $\mu\text{M}$ . Finally, real-time fluorescence observation was observed to evaluate the efficiency of both complexes for probing the nuclei of living tumor cells. Thus, the characterized red fluorescence ascribed to these complexes gradually intensified in the nuclei of the various cell lines during incubation. The strongest intensity was observed at 90 min, which was maintained until 120 min. This characteristic was further confirmed by the decrease in the amounts of **1** and **2** in the cells culture medium. Therefore, both **1** and **2** can be used as novel fluorescence probes in imaging of the nuclei of living tumor cells. In addition, **1** and **2** were

also distinguished. The hydrophobicity of ancillary ligands plays a key role in promoting the penetration of a complex into the membrane. Complexes with high hydrophobicity are generally easily uptaken by cells.<sup>19,21,24–27</sup> In our studies, the octanol/water partition coefficients ( $\log P$ ) obtained for **1** and **2** were approximately 0.18 and 0.10, respectively. These results were consistent with the reported values.<sup>50</sup> In summary, a method has been constructed to develop novel fluorescence probes in targeting imaged nuclei of living tumor cells using ruthenium(II) complexes coordinated with CQM. The detailed mechanism of these complexes are under further investigations.

## 5 Conclusions

In summary, two novel ruthenium(II) complexes coordinated with 6-chloro-5-hydroxypyrido[3,2-*a*]phenazine (CQM),  $[\text{Ru}(\text{L})_2(\text{CQM})]\text{ClO}_4$  (L = phen, **1**; and bpy, **2**), have been synthesized. It's demonstrated that both complexes can be uptaken by tumor cells, with **1** localized mainly in the nuclei, while **2** accumulated in the mitochondria and nuclei of HepG2 cells. The further studies by real time fluorescence observations show that both **1** and **2**, especially **1** can be used to image the nuclei of living tumor cells. In a word, this kind of complexes may be developed as low toxicity fluorescence probe of tumor cells in the future.

## Acknowledgements

This works was supported by the National Nature Science Foundation of China (81373257), the Provincial Major Scientific Research Projects in Universities of Guangdong Province (2014KZDXM053), the Science and Technology Item Foundation of Guangzhou

(2013J4100072) and the Joint Natural Sciences Fund of the Department of Sciences and Technology & the First Affiliated Hospital of Guangdong Pharmaceutical University (GYFYLH201309).

## References

- 1 B. Valeur and M. N. Berberan-Santos, John Wiley & Sons., 2012.
- 2 P. Urayama, W. Zhong, J. A. Beamish, F. K. Minn, R. D. Sloboda, K. H. Dragnev, E. Dmitrovsky and M. A. Mycek, *Applied Physics B.*, 2003, **76**, 483-496.
- 3 Z. Zhang and S. Achilefu, *Org. Let.*, 2004, **6**, 2067-2070.
- 4 W. Zhong, P. Urayama and M. A. Mycek, *J. Phys. D: App. Phys.*, 2003, **36**, 1689.
- 5 E. Musatkina, H. Amouri, M. Lamoureux, T. Chepurnykh and C. Cordier, *J. Inorg. Biochem.*, 2007, **101**, 1086-1089.
- 6 K. K. W. Lo, K. H. K. Tsang, K. S. Sze, C. K. Chung, T. K. M. Lee, K. Y. Zhang, W. K. Hui, C. K. Li, J. S. Y. Lau, D. C. M. Ng and N. Zhu, *Coord. Chem. Rev.*, 2007, **251**, 2292-2310.
- 7 L. F. Tan, L. J. Xie and X. N. Sun, *J. Biol. Inorg. Chem.*, 2013, **18**, 71-80.
- 8 C. J. Murphy, M. R. Arkin, N. D. Ghatlia, S. Bossmann, N. J. Turro and J. K. Barton, *PNAS.*, 1994, **91**, 5315-5319.
- 9 H. A. Wagenknecht, E. D. A. Stemp and J. K. Barton, *J. Am. Chem. Soc.*, 2000, **122**, 1-7.
- 10 R. M. Hartshorn and J. K. Barton, *J. Am. Chem. Soc.*, 1992, **114**, 5919-5925.
- 11 J. W. Dobrucki and J. Photochem, *Photobiol. B: Biol.*, 2001, **65**, 136-144.

- 12 F. R. Svensson, J. Andersson, H. L. Amand and P. Lincoln, *J. Biol. Inorg. Chem.*, 2012, **17**, 565-571.
- 13 V. Pierroz, T. Joshi, A. Leonidova, C. Mari, J. Schur, I. Ott, L. Spiccia, S. Ferrari and G. Gasser, *J. Am. Chem. Soc.*, 2012, **134**, 20376-20387.
- 14 J. Q. Wang, P. Y. Zhang, C. Qian, X. J. Hou, L. N. Ji and H. Chao, *J. Biol. Inorg. Chem.*, 2014, **19**, 335-348.
- 15 J. X. Zhang, J. W. Zhou, C. F. Chan, T. C. K. Lau, D. W. Kwong, H. L. Tam, N. K. Mak, K. L. Wong and W. K. Wong, *Bioconj. Chem.*, 2012, **23**, 1623-1638.
- 16 M. R. Gill, D. Cecchin, M. G. Walker, R. S. Mulla, G. Battaglia and C. Smythe, J. A. Thomas, *Chem. Sci.*, 2013, **4**, 4512-4519.
- 17 A. E. Friedman, J. C. Chambron, J. P. Sauvage, N. J. Turro and J. K. Barton, *J. Am. Chem. Soc.*, 1990, **112**, 4960-4962.
- 18 E. J. C. Olson, D. Hu, A. Hörmann, A. M. Jonkman, M. R. Arkin, E. D. A. Stemp, J. K. Barton and P. F. Barbara, *J. Am. Chem. Soc.*, 1997, **119**, 11458-11467.
- 19 C. A. Puckett and J. K. Barton, *J. Am. Chem. Soc.*, 2007, **129**, 46-47.
- 20 C. A. Puckett and J. K. Barton, *Biochem.*, 2008, **47**, 11711-11716.
- 21 V. Rajendiran, M. Palaniandavar, V. S. Periasamy and M. A. Akbarsha, *J. Inorg. Biochem.*, 2012, **116**, 151-162.
- 22 V. Rajendiran, M. Palaniandavar, V. S. Periasamy and M. A. Akbarsha, *J. Inorg. Biochem.*, 2010, **104**, 217-220.

- 23 N. Deepika, Y. P. Kumar, C. S. Devi, P. V. Reddy, A. S. Srishailam and S. Satyanarayana, *J. Biol. Inorg. Chem.*, 2013, **18**, 751-766.
- 24 M. Matson, F. R. Svensson, B. Nordén and P. Lincoln, *J. Phys. Chem. B.*, 2011, **115**, 1706-1711.
- 25 F. R. Svensson, M. Matson, M. Li and P. Lincoln, *Biophys. Chem.*, 2010, **149**, 102-106.
- 26 C. A. Puckett and J. K. Barton, *J. Am. Chem. Soc.*, 2009, **131**, 8738-8739.
- 27 U. Neugebauer, Y. Pellegrin, M. Devocelle, R. Forster, W. Signac, N. Moran and T. E. Keyes, *Chem. Comm.*, 2008, 5307-5309.
- 28 K. K. W. Lo, T. K. M. Lee, J. S. Y. Lau, W. L. Poon and S. H. Cheng, *Inorg. Chem.*, 2008, **47**, 200-208.
- 29 M. J. Pisani, D. K. Weber, K. Heimann, J. G. Collins and F. R. Keene, *Metallomics.*, 2010, **2**, 393-396.
- 30 M. J. Pisani, P. D. Fromm, Y. Mulyana, R. Clarke, H. Körner, P. K. Heimann, J. G. Collins and Keene F R, *Chem. Med. Chem.*, 2011, **6**, 848-858.
- 31 A. M. Pyle and J. K. Barton, *Progress in Inorganic Chemistry: Bioinorg. Chem.*, 1990, **38**, 413-475.
- 32 Y. Cheng, L. K. An, N. Wu, X. D. Wang, X. Z. Bu, Z. S. Huang and L. Q. Gu, *Bioorg. Med. Chem.*, 2008, **16**, 4617-4625.
- 33 W. Zhang, Q. M. Chen, X. Cheng, N. Wu, G. B. Yi, D. Li, J. H. Tan, Z. S. Huang, L. Q. Gu and L. K. An, *Dyes and Pigments.*, 2013, **99**, 82-89.
- 34 B. A. Roberts and C. R. Strauss, *Acc. Chem. Res.*, 2005, **38**, 653-661.

- 35 R. Hoogenboom and U. S. Schubert, *Macromol. Rap. Comm.*, 2007, **28**, 368-386.
- 36 V. Polshettiwar and R. S. Varma, *Acc. Chem. Res.*, 2008, **41**, 629-639.
- 37 Q. Wu, C. D. Fan, T. F. Chen, C. R. Liu, W. J. Mei, S. D. Chen, B. G. Wang, Y. Y. Chen and W. J. Zheng, *Eur. J. Med. Chem.*, 2013, **63**, 57-63.
- 38 Q. Wu, T. F. Chen, Z. Zhang, S. Y. Liao, X. H. Wu, J. Wu, W. J. Mei, Y. H. Chen, W. L. Wu, L. L. Zeng and W. J. Zheng, *Dalton Trans.*, 2014, **43**, 9216-9225.
- 39 Z. Zhang, Q. Wu, X. H. Wu, F. Y. Sun, L. M. Chen, J. C. Chen, S. L. Yang and W. J. Mei, *Eur. J. Med. Chem.*, 2014, **80**, 316-324.
- 40 Z. Zhang, Y. J. Wang, Q. Wu, X. H. Wu, F. Q. Sun, B. G. Wang, W. J. Mei and S. D. Chen, *Aust. J. Chem.*, 2015, **68**, 137-144.
- 41 R. Pagadala, P. Ali and J. S. Meshram, *J. Coord. Chem.*, 2009, **62**, 4009-4017.
- 42 S. Rau, B. Schäfer, A. Grüßing, S. Schebesta, K. Lamm, J. Vieth, H. Gorls, D. Walther, M. Rudolph, U. W. Grummt and E. Birkner, *Inorg. Chim. Acta.*, 2004, **357**, 4496-4503.
- 43 M. R. Gill and J. A. Thomas, *Chem. Soc. Rev.*, 2012, **41**, 3179-3192.
- 44 C. Hiort, P. Lincoln and B. Norden, *J. Am. Chem. Soc.*, 1990, **115**, 3448-3454.
- 45 A. E. Friedman, J. C. Chambron, J. P. Sauvage, N. J. Turro and J. K. Barton, *J. Am. Chem. Soc.*, 1990, **112**, 4960.
- 46 Y. Jenkins, A. E. Friedman, N. J. Turro and J. K. Barton, *Biochem.*, 1992, **31**, 10809.
- 47 J. Olofsson, B. Onfelt and P. Lincoln, *J. Phys. Chem. A.*, 2004, **108**, 4391.
- 48 M. Ardhammer, P. Lincoln and B. Norden, *J. Phys. Chem. B.*, 2001, **105**, 11363.
- 49 B. Onfelt, L. Gostring, P. Lincoln, B. Norden and A. Onfelt, *Mutagenesis.*, 2002, **17**, 317-

320.

50 M. R. Gill, H. Derrat, C. G. W. Smythe, G. Battaglia and J. A. Thomas, *Chem. Bio.*

*Chem.*, 2011, **12**, 877-880.

## Figure Captions

**Scheme 1.** Molecular structure of ruthenium(II) complexes **1** and **2**.

**Figure 1.** (A) Fluorescence of **1** and **2** in EtOH, DMEM, and PBS buffer solution (pH 7.2) excited at 365 nm from a portable lamp. [Ru] = 100  $\mu$ M. (B) Electronic spectra and emission spectra ( $\lambda_{\text{ex}} = 400$  nm) of **1** and **2** in Tris-KCl buffer solution (pH 7.2). [Ru] = 100  $\mu$ M. (C) Images of confocal laser scanning microscopy of HepG2 cells incubated with **1** and **2**. Cells were treated with ruthenium(II) complexes for 2 h at 37 °C. Blue: Hoechst, Green: Mito-tracker green. [Ru] = 200  $\mu$ M. (D) A cross sectional compositional line profile of a single cell of **1** and **2** emission intensity under confocal laser scanning microscopy image.

**Figure 2.** Cellular uptake of **1** and **2** in HepG2 (A), HeLa, (B) and MCF-7 (C) cells by fluorescence microscopy. Cells treated with either **1** or **2** ([Ru] = 200  $\mu$ M) in PBS (1% DMSO, pH 7.2) for 2 h at 37 °C, followed by 2  $\mu$ g/mL DAPI for 10 min. Luminescence intensity of complexes **1** and **2** in the HepG2 (a), HeLa (b), and MCF-7 (c).

**Figure 3.** In vitro cell viabilities of HepG2 (A), HeLa (B), MCF-7 (C), and HaCaT (D) cells incubated with **1** and **2** at 37 °C for 24h.

**Figure 4.** Real-time fluorescence observation of HepG2 (A), HeLa (B), and MCF-7 (C) cells after treatment by **1** or **2** (200  $\mu$ M) in DMSO and PBS (pH 7.2, 1:99, v/v) for 2 h at 37 °C. Time course of the transfection rates of **1** and **2** in HepG2 (a), HeLa (b), and MCF-7 (c) cells. Time dependence of changes in concentration of ruthenium(II) complexes **1** and **2** detected by UV-vis absorbance of (D) HepG2, (E) HeLa, (F) MCF-7 cells; (G) Octanol/water partition coefficients of ruthenium(II) complexes **1** and **2** at room temperature.

Scheme 1

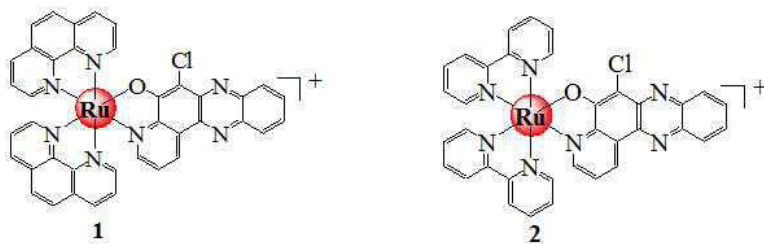


Figure 1

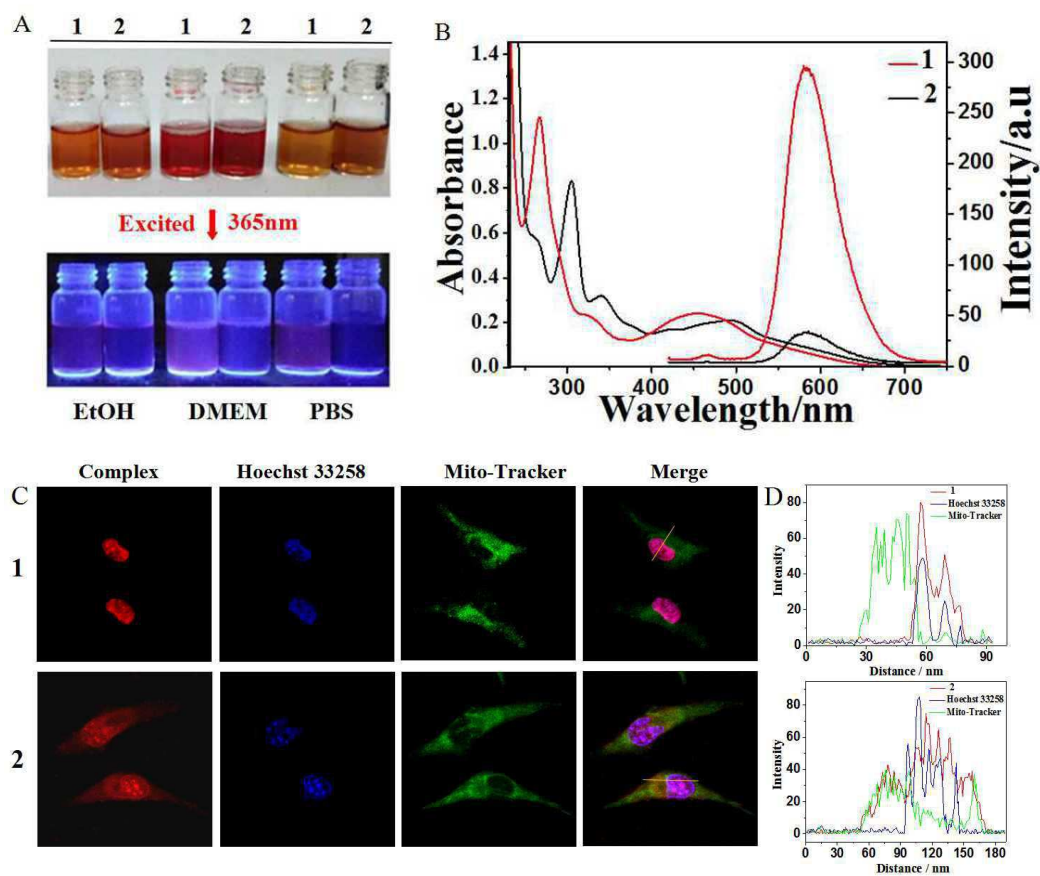


Figure 2

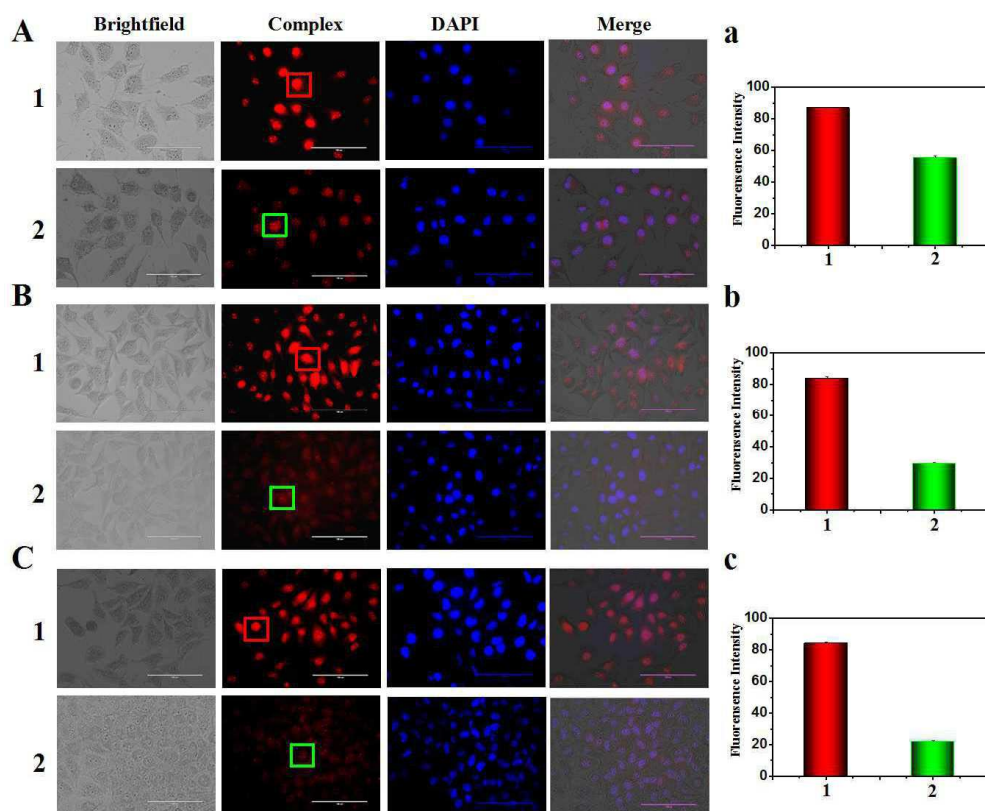


Figure 3

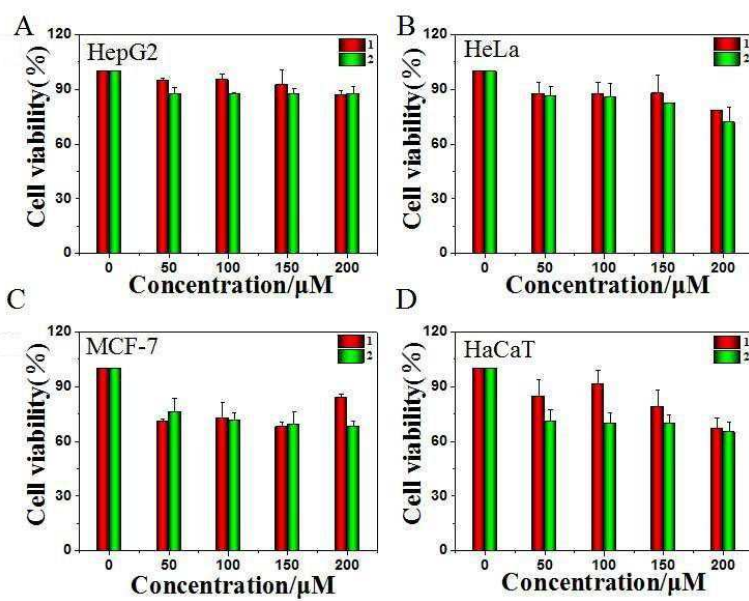
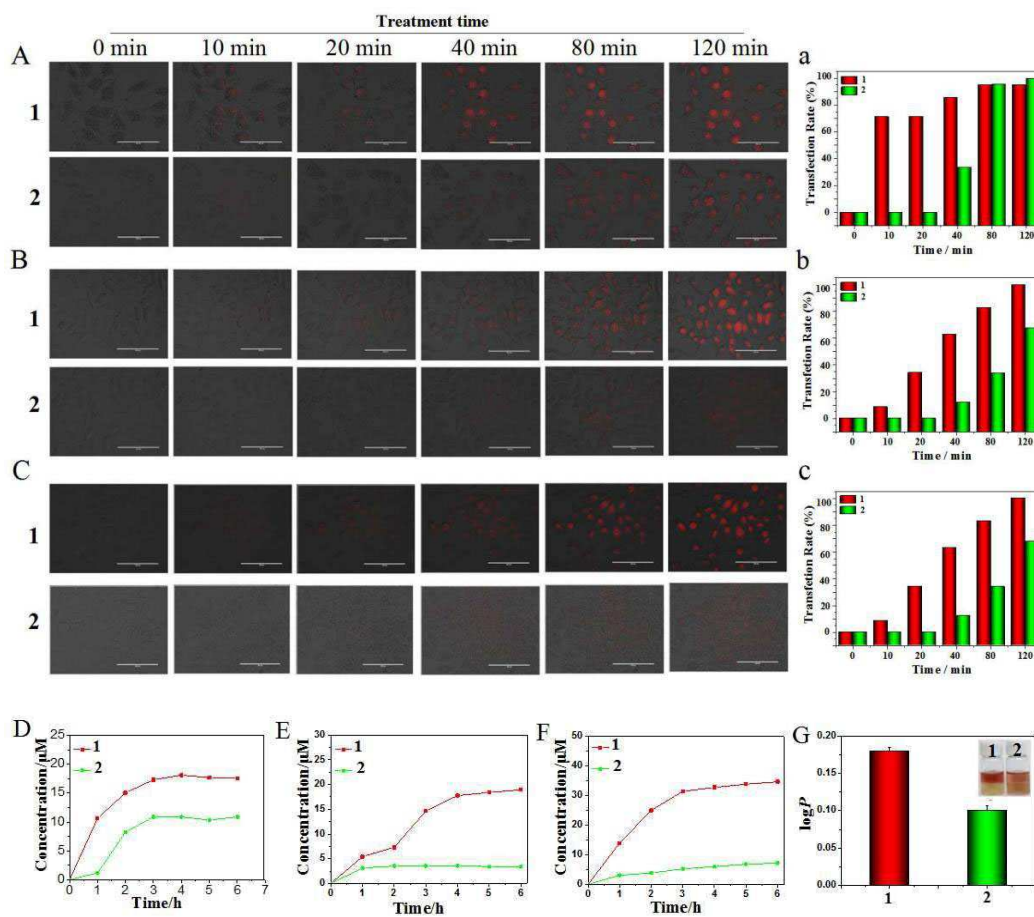


Figure 4



## Graphic abstract

The novel ruthenium(II) complex **1** can be developed as low toxicity fluorescence probe for living cell nucleus in the future.

